ORIGINAL ARTICLE

rpth
research & practice in thrombosis & haemostasis

Epitope of antiphospholipid antibodies retrieved from peptide microarray based on R39-R43 of β2-glycoprotein I

Marc Moghbel MSc[1] | Aline Roth[2] | Daniela Baptista PhD[2] |
Kapka Miteva PhD[2] | Fabienne Burger MSc[2] | Fabrizio Montecucco MD[3,4] |
Nicolas Vuilleumier MD[5,6] | François Mach MD[2] | Karim J. Brandt PhD[1,2]

[1]Endotelix Diagnostics Sàrl, Geneva, Switzerland

[2]Division of Cardiology, Department of Medicine, Faculty of Medicine, Foundation for Medical Research, University of Geneva, Geneva, Switzerland

[3]Ospedale Policlinico San Martino Genoa, Italian Cardiovascular Network, Genoa, Italy

[4]Department of Internal Medicine and Centre of Excellence for Biomedical Research (CEBR), First Clinic of Internal Medicine, University of Genoa, Genoa, Italy

[5]Department of Genetic Medicine, Laboratory and Pathology, Geneva University Hospitals, Geneva, Switzerland

[6]Division of Laboratory Medicine, Faculty of Medicine, University of Geneva, Geneva, Switzerland

Correspondence
Karim J. Brandt, Division of Cardiology, Department of Internal Medicine, Faculty of Medicine, Foundation for Medical Research, University of Geneva, Av de la Roseraie 64, CH-1211 Geneva 14, Switzerland.
Email: karim.brandt@unige.ch

Abstract

Background: Antiphospholipid antibody (aPL) syndrome (APS) is an autoimmune disease characterized by the presence of antiphospholipid antibodies and thromboembolic or pregnancy complications. Although cryptic epitope R39-R43 belonging to beta-2-glycoprotein 1 (β2GP1) has been identified as the main antigenic determinant for aPLs, we have recently demonstrated that the epitope is a motif determined by the polarity, rather than by the sequence or charge of amino acids.

Objective: In the present study, we wanted to identify the association of residues needed to obtain the highest aPL affinity.

Methods: Based on the epitope R39-R43 and our identified motif, we generated a printed peptide microarray of 676 different peptides. These peptides have been then screened for their ability to interact with the plasmas from 11 well-characterized APS patients and confirmed by surface plasma resonance assay.

Results and Conclusions: We identified a peptide that selectively bound immunoglobulin G (IgG) derived from APS patients with 100 times more affinity than β2GP1, Domain I, or epitope R39-R43. This peptide is able to inhibit the activity of IgG derived from APS patients in vitro. We have also generated a monoclonal IgG antibody against this peptide. Using both peptide and monoclonal antibody, we have been able to develop a fully standardized indirect colorimetric immunoassay with highly sensitivity. The identification of the optimized peptide offers a new standardized and accurate tool for diagnostics of APS. Furthermore, having increased affinity for aPL, this peptide could represent a useful tool as prevention strategy for APS and an alternative to the use of anticoagulants.

KEYWORDS
β2GP1, antibody, antiphospholipid syndrome, ApoH, autoimmune disease, ELISA, epitope, pregnancy complications, systemic lupus erythematosus, thrombosis

Essentials

- Antiphospholipid antibodies (aPL) contribute to abnormal clotting risk.
- Exact aPL-binding site on their targets are not well defined
- We found a peptide with strong binding to aPL and ability to block aPL.
- This peptide offers a new standardized and accurate tool for diagnosing aPL

1 | INTRODUCTION

Antiphospholipid syndrome (APS) is described as a common risk factor for recurrent thromboembolic events and/or pregnancy complications resulting from circulating antiphospholipid antibodies (aPL).[1] APS may be concomitant with systemic lupus erythematosus (SLE), other autoimmune diseases, malignant diseases, and bacterial or viral infections (secondary APS) but may also occur without an underlying disease (primary APS).

β2GP1 is a protein of 43 kDa composed of five short consensus repeat domains called "sushi" domains and is considered to be the main antigenic target for aPL.[2] At least two different conformations are known for β2GP1: a circular plasma conformation in which domain I interacts with domain V and an "activated" fishhook-like conformation. The fishhook-like conformation is obtained after binding of positively charged patch of domain V to anionic phospholipids. The dissociation of domain I and domain V leads to the exposure of an epitope containing the amino acids Arg39 and Arg43 that are critical for binding of pathogenic aPL.[3,4] This cryptic epitope is described as being located around residues 39 and 43; however, Iverson et al. have identified additional surrounding residues involved in the recognition of pathogenic anti-β2GP1 IgG antibodies in domain I.[5,6] Our research group has recently shown that the immunodominant β2GP1-specific CD4$^+$ T-cell epitope shares a common peptide motif present in the β2GP1 peptide sequence R39-R43.[7] We have further determined that the characteristic ΦΦΦζζFxC motif, in which Φ represents nonpolar residues (AVILMFWCPG) and ζ polar residues (YTSHKREDQN), as well as motifs closely related to ΦΦΦζζFxΦ are present several times in β2GP1 but also in every receptor described for aPL.[7,8] We have also suggested that additional developments should be necessary to find the exact association of residues needed to obtain the highest aPL affinity. We present here the investigations leading to identifying a new sequence of amino acids relative to R39-R43 and peptide motif ΦΦΦζζFxΦ, given a stronger affinity for aPL from APS patients. We demonstrate the space-oriented requirement of this peptide for proper interaction with aPL. This study offers the opportunity to provide an accurate tool to detect anti-β2GP1 IgG antibodies for diagnostic purposes. It also represents a strong base for the development of effective, specific, and safe treatment for APS patients.

2 | METHODS

2.1 | Ethical statement

All breeding and experimental protocols and procedures were reviewed and approved by the Institutional Animal Care and Use Committee of the Geneva University School of Medicine. Animal care and experimental procedures were carried out in accordance with the guidelines of the Institutional Animal Care and Use Committee of the Geneva University School of Medicine and complied with the guidelines from Directive 2010/63/EU of the European Parliament on the protection of animals used for scientific purposes. All data generated or analyzed during this study are included in this published article (and in Appendix S1).

2.2 | Patient characteristics

All patients had APS, as defined by the revised Sapporo criteria. Blood was obtained from each patient with written consent and approval by the institutional ethics committee of the University Hospital of Geneva. In accordance with the decision of the 7 April 2014 of the Cantonal Research Ethics Committee of the Geneva (ccer@etat.ge.ch), all experimental protocols were approved under protocol 09-072 entitled "Pathogenic effects of antiphospholipid antibodies," and with the Declaration of Helsinki, the blood bank obtained informed consent from the donors, who were informed that part of their blood would be used for research purposes. The characteristics of the patients enrolled in this study have been partially presented in previous publications[7,9] and resume in Table S1. The pooled plasma used in the present study is a mix of 11 plasma samples.

2.3 | Mice

B6.Nba2.*Yaa* mice were generated as described.[10] The Apoe$^{-/-}$ null mutation was introduced in B6.Nba2.*Yaa* mice by breeding. Eleven-week-old Apoe$^{-/-}$ C57Bl/6 and Apoe$^{-/-}$Nba2.*Yaa* mice were subjected to 11 weeks of a high cholesterol diet (20.1% fat, 1.25% cholesterol; Research Diets, Inc.) as a model of advanced atherosclerosis. The treatments and atherosclerosis protocols were well-tolerated by the mice, and no adverse events (such as weight loss and signs of systemic toxicity) were reported. At sacrifice, hematological parameters were routinely measured. Animals were euthanized by exsanguination after anesthesia with 4% isoflurane.

2.4 | Microarray

The peptide microarray was performed blinded by PEPperPRINT GmbH, Heidelberg, as follow: prestaining of a peptide microarray

was done with secondary goat anti-human immunoglobulin G (IgG) (H+L) DyLight680 antibody (1:5000) and control mouse monoclonal anti-HA (12CA5) DyLight800 antibody (1:2000) to investigate background interactions with the variants of wild-type peptide that could interfere with the main assays. Subsequent incubation of other peptide microarray copies with human antibodies at concentrations of 100 μ/ml and 500 μg/ml in incubation buffer was followed by staining with secondary and control antibodies as well as readout at scanning intensities of 7/7 (red/green). The control staining of the HA epitopes was done as internal quality control to confirm the assay quality and the peptide microarray integrity. Quantification of spot intensities and peptide annotation were based on the 16-bit grayscale tiff files at scanning intensities of 7/7 that exhibit a higher dynamic range than the 24-bit colorized tiff files; microarray image analysis was done with PepSlide Analyzer. A software algorithm breaks down fluorescence intensities of each spot into raw, foreground, and background signals, and calculates averaged median foreground intensities and spot-to-spot deviations of spot triplicates. Based on averaged median foreground intensities, an intensity map was generated and interactions in the peptide map highlighted by an intensity color code with red for high and white for low spot intensities. We tolerated a maximum spot-to-spot deviation of 40%; otherwise, the corresponding intensity value was zeroed.

2.5 | Immunoassays

2.5.1 | Determination of aPL by ELISA

MaxiSorp 96 well plates (Nunc) or Pierce streptavidin-coated high-capacity 96-well plates (Thermofisher) were coated with 10 μg/ml recombinant domains of β2GP1, oxidized β2GP1, peptides, or biotinylated-peptide before incubation with aPL. Secondary anti-human antibodies conjugated to IR800CW (Rockland) or horseradish peroxidase were used. Protein- or peptide-bound antibodies were detected and quantified by the Odyssey system (Li-Cor Biosciences) (fluorescence is expressed on arbitrary unit [AU]) or absorbance in optical densities was determined at 405 nm (Molecular Devices Filtermax). For the calculation of 99th percentile, we measured with our immunoassay for anti-β2GP1 IgG (anti-IIa-8.0-2x) levels from 236 healthy donors (blood bank donors). Mean age of the donors was 47 years, and 83.5% were female (Table S2).

2.5.2 | Determination of autoantibodies anti-apoA-1 by ELISA

Maxisorp plates (Nunc) were coated with purified, derived delipidated murine recombinant apolipoprotein A-1 (Biorbyt) (20 mg/ml; 50 ml/well) for 1 h at 37°C. After washing, all wells were blocked for 1 h with 2% bovine serum albumin (BSA) in phosphate buffered solution at 37°C. Then, samples were incubated for 1 h. Samples were also added to a noncoated well to assess individual nonspecific

binding. After washing, 50 μl/well of signal antibody (alkaline phosphatase-conjugated anti-human IgG; Sigma-Aldrich) diluted 1:1000 in phosphate buffered solution/bovine serum albumin 2% solution was incubated 1 h at 37°C. After washing, phosphatase substrate p-nitrophenyl phosphate disodium (Sigma-Aldrich) dissolved in diethanolamine buffer (pH 9.8) was added. Each sample was tested in duplicate and absorbance in optical densities was determined at 405 nm after 20 min of incubation at 37°C (Molecular Devices TM Filtermax). Corresponding nonspecific binding was subtracted from mean absorbance for each sample.

2.5.3 | Determination of autoantibodies anti-dsDNA by ELISA

Salmon sperm dsDNA was coated to ELISA plates precoated with poly-L-lysine (Sigma-Aldrich). Plates were then incubated with 1/100 diluted serum samples, and development performed with alkaline phosphatase-labeled goat anti-mouse IgM or IgG. Results are expressed in U/ml in reference to a standard curve.

2.6 | Surface plasmon resonance

The kinetics and affinity of protein–protein and protein–lipid interactions were determined using a BIAcore X100 instrument. A total of 1 mg/ml of biotin-tagged peptide (ligand) was immobilized using a sensor chip SA (GE Healthcare) surface, whereas aPL from a pool of plasma from 11 human patients was used as analyte. The first flow cell of the sensor chip was used as a control surface (no protein), whereas the second flow cell was used as the active surface. A range of dilution of aPL analytes prepared in the same buffer was injected on both flow cell surfaces at a flow rate of 30 μl/min. Association and dissociation times for each protein injection were set at 90 and 120 s, respectively. In all cases, sensorgrams were obtained from three different dilutions of aPL, and K_d has been determined when the concentration of analytes was known.

2.7 | Monoclonal IgG production

Monoclonal IgG has been generated by GenScript Biotech B.V. following their MonoExpress protocol from our peptide anti-IIa-8.0-biot-2x. The production has then upscaled to produce large amount of antibody with <3 EU/mg of endotoxin.

2.8 | Inhibition experiments

To assess the ability of IIa-5.0-2x, IIa-7.1-2x, and IIa-8.0-2x to inhibit in vitro the binding of aPL to IIa-8.0-biot-2x. aPL pool sera were preincubated for 90 min at room temperature with increasing concentrations (1, 10, and 100 μg/ml) of monomeric, dimeric

IIa-5.0, IIa-7.1, and IIa-8.0 peptides and of IIa-5.0-biot-2x, IIa-7.1-biot-2x, and IIa-8.0-biot-2x-associated beads (15, 30, and 60 pmol). A total of 120 pmol corresponded to the amount of IIa-8.0-biot-2x coated in well of streptavidin-coated high-capacity 96-well plates (Thermofisher). After the preincubation time, the serum was added to anti-β2GP1 IgG (anti-IIa-8.0-2x) ELISA according to the protocol.

2.9 | Sequences alignment

All the downloaded protein sequences were aligned using the Clustal Omega – Multiple Sequence Alignment program with default settings.[11]

2.10 | Statistical analysis

Statistics were performed using GraphPad Prism 8, Statistica (version 13.0). Data are presented as mean ± standard error of the mean (SEM). For clinical scores, significance between groups was analyzed using the nonparametric Mann–Whitney U test. Spearman rank correlation coefficients were used to assess correlations between variables. The number of mice used for each analysis is indicated in the figure legends. All data are presented as the mean ± SEM and the statistical significance threshold used is $*p \leq 0.05$; $**p \leq 0.05$; $***p \leq 0.005$.

3 | RESULTS

3.1 | Epitope R39-R43 is only a part of the epitope-determining sequence for aPL

Although our recent study has led to the determination of an antiphospholipid antibody-interacting motif as φφφζζFxφ, we have also suggested that the exact association of residues on the peptide could provide the highest aPL affinity for the epitope.[7] We have thus performed a peptide substitution scan of wild-type peptide VSR<u>GGMRKFIC</u>PLTG carrying the epitope R39-R43 and based on an exchange of the underlined amino acid positions with the 20 main amino acids. The resulting peptide microarrays contained 136 different peptides. Although the substitution does not fully follow the rules of the motif described previously, we can observe that the peptide substitution for the positions 4–10 (Figure 1A) have no real influences on its ability to interact with aPL neither from patients 1, 2, 3, or 4 nor the pool of plasma whose characteristics are shown in Table S1. However, the substitution of the position 11 by an arginine (R) and, in particular, a lysine (K) increases the affinity of the peptide for four aPLs and the pool of patients (Figure 1A). Although the substitution of the position 11 by a Lys shows a stronger interaction with aPL, we decided to perform a second peptide substitution scan on the VSRGGMRK<u>FI</u>KPLTG based on an exchange of the underlined amino acid positions with the 20 main amino acids

to identify a potential additional improvement of the affinity for aPL. The microarrays contained 400 different peptides. Within this library, we noticed, however, that the residue present in position 9 has a strong influence on the affinity of aPL. Although the presence of a lysine or arginine in position 9 with different residues in position 10 could have some positive effects on the interaction with aPL, the association of lysine and arginine to positions 9 and 10 leads to a robust binding to aPL (Figures 1B, 2A–C). It appears, however, that the combination of two lysines in positions 9 and 10 have the strongest affinity for aPL (Figure 2A). These results demonstrate that the core sequence of the β2GP1-derived peptide embedded R39-R43 epitope and four lysines next to arginine 43.

### 3.2 | Epitope recognized by aPL requires to be spatially oriented for optimal interactions

To compare the ability of β2GP1, domain I-II of β2GP1, R39-R43 peptide, and Ia-1 peptide corresponding to the first substitution scan (Figure 1) and Ib-1 peptide and corresponding to the second substitution scan (Figure 2) to bind to aPL, we performed a custom immunoassay. We took the binding level of aPL to β2GP1 as reference (Figure 3A,B). We can see that Dom I-II and R39-R43 have the same ability to interact with aPL than β2GP1, whereas the interaction of Ia-1 and Ib-1 peptide have an increased fold mean time of 3.47 and 5.5, respectively (Figure 3A). The de Groot research group has pointed at the importance of hydrophobic character of the plate during coating of R39-R43 epitope.[12] To abrogate of the plate-dependent aPL binding, we synthesized the Ia-1 and Ib-1 peptide as well as the R39-R43 with a biotin at their N-terminal and coated a streptavidin plate. In this configuration, the different peptides are flag oriented in the space, preventing any interaction with the plate. We can thus observe that the flag-type orientation of R39-R43-biot leads to 8.52× more interaction with aPL, whereas they show 9.63× more binding for Ib-1-biot presenting the same position. The interactions remain 2.83× and 4.3× with R39-R43-biot and Ib-1-biot, respectively, after a dilution of 100× of aPL (Figure 3B). The surface plasmon resonance (SPR) technique is used to determine the relative affinity of aPL for R39-R43-biot and Ib-1-biot. The interaction between aPL and immobilized R39-R43-biot or Ib-1-biot is monitored by flowing various concentrations of aPL over a R39-R43-biot- or Ib-1-biot-coated chip surface (Figure 3C). Through SPR experiments, it appears that aPL affinity for Ib-1-biot presents a resonance unit (RU) of 51.49 at 1/1000 of dilution and an RU of 27.61 at 1/10,000 of dilution whereas, at the same dilution, it presents an RU of 27.36 and an RU of 17.99 with R39-R43-biot, respectively (Figure 3C). However, at higher concentrations, the peptides seem to show no differences in the interactions with aPL. We can further observe that neither R39-R43-biot nor Ib-1-biot have sustained interaction with aPL considering the stabilization curves. Considering IgG valency, we decided to generate a dimeric Ib-1-biot peptide (Ib-1-biot-2x). This new polypeptide thus carries two high-affinity epitopes that have the opportunity to interact with two Fab
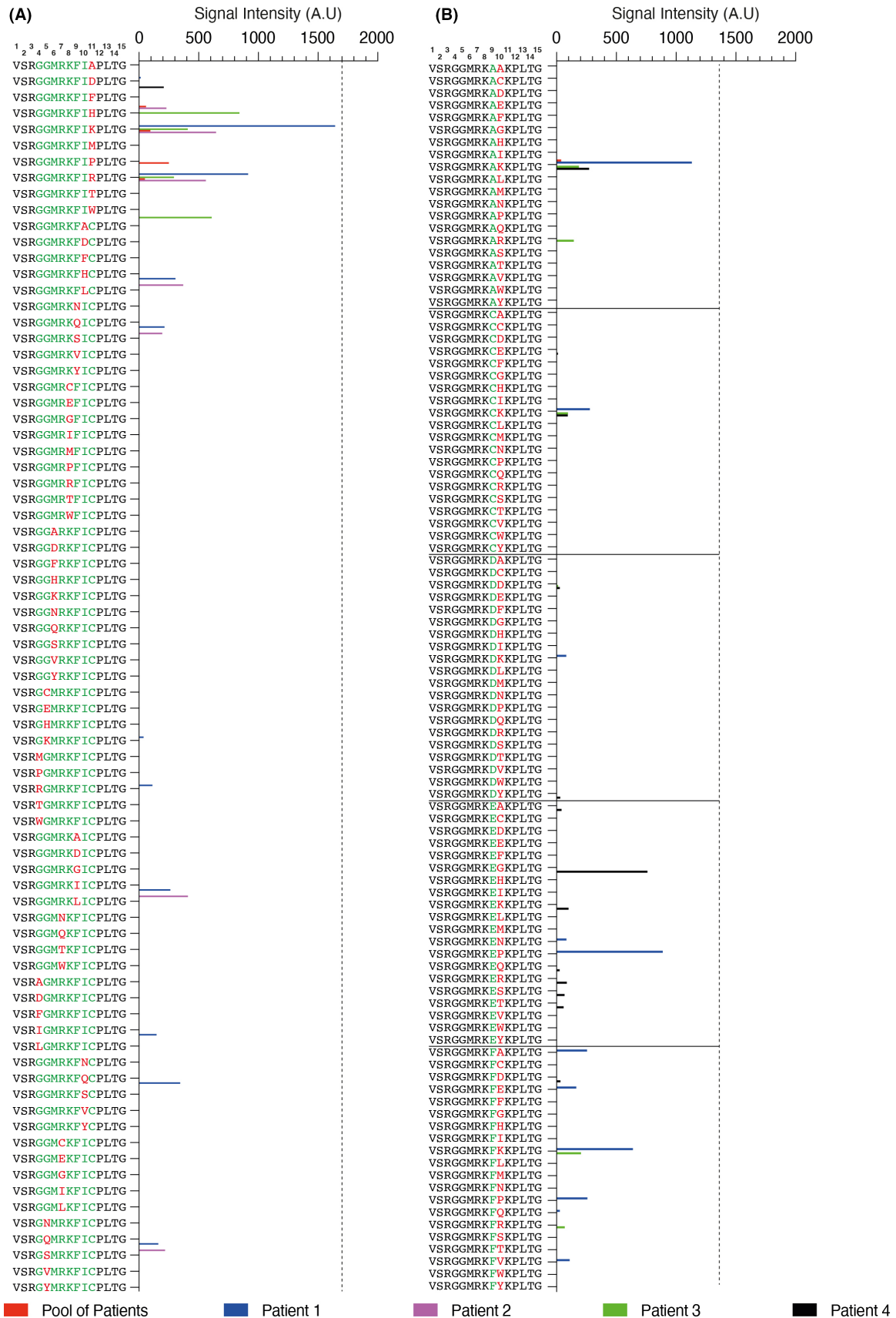
FIGURE 1 Epitope R39-R43 is only a part of the epitope-determining sequence for aPL. (A) Graphical representation of a peptide substitution scan microarray performed on VSR<u>GGMRKFIC</u>PLTG and (B) VSRGGMRKF<u>I</u>KPLTG with four different aPLs (patients 1, 2, 3, and 4) and a pool of 11 patients (Pool) at 500 µg/ml
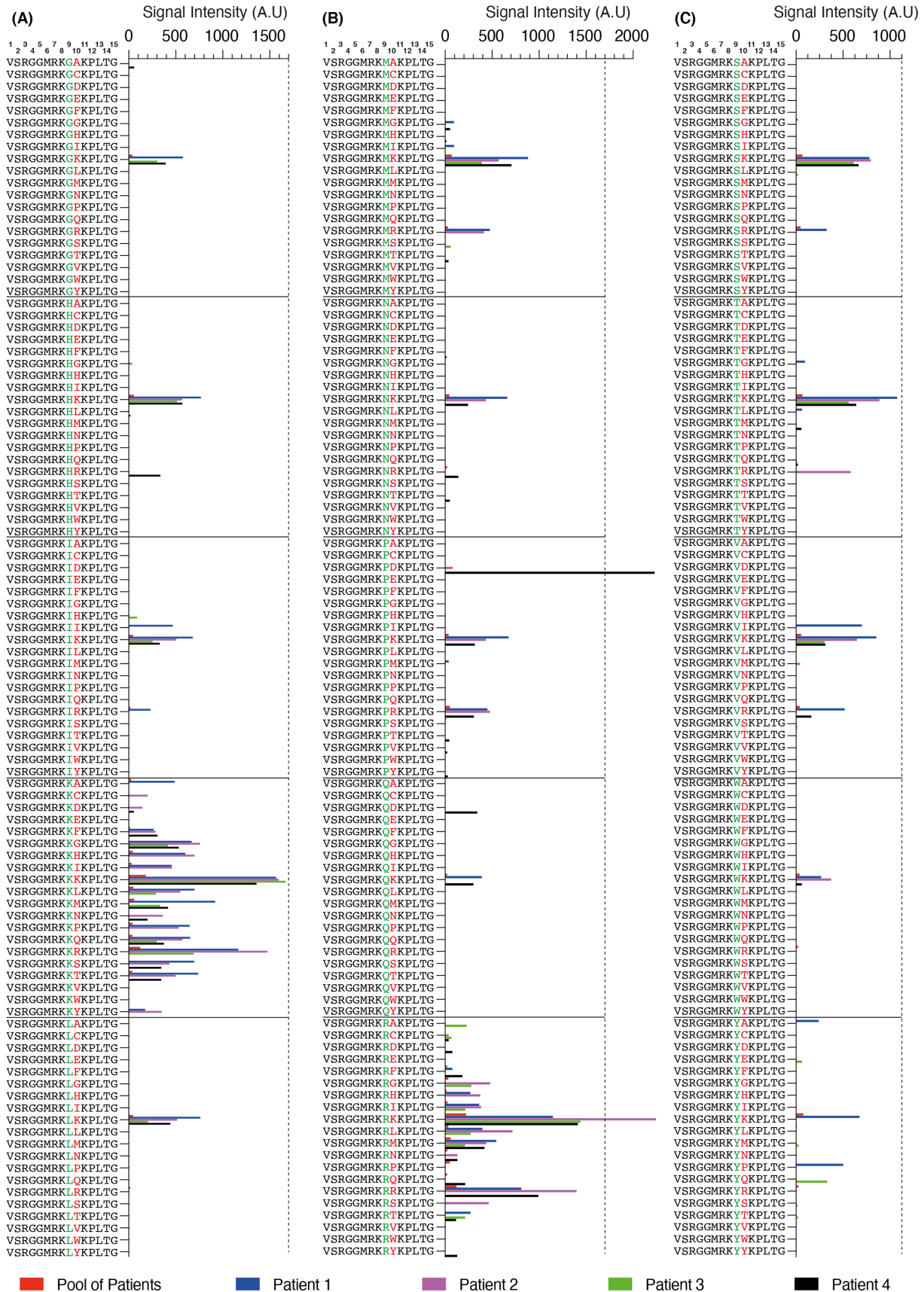
FIGURE 2 Lysine (K) and arginine (R) are determinants for aPL interactions. (A–C) Graphical representation of a peptide substitution scan microarray performed on VSRGGMRK FIKPLTG with four different aPLs (patients 1, 2, 3, and 4) and a pool of 11 patients (Pool) at 500 μg/ml

(A)

Identified Peptides

R39-R43 ^{1}VSRGGMRKFICPLTG^{15}
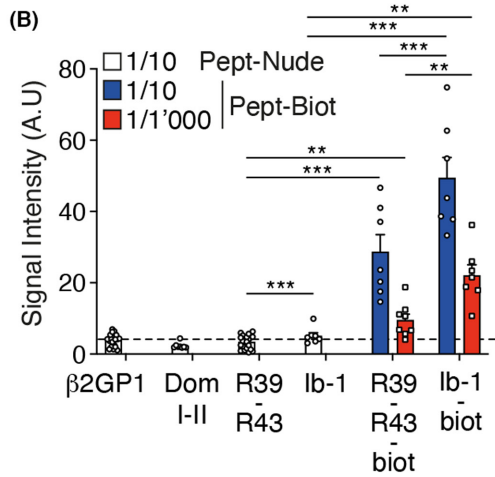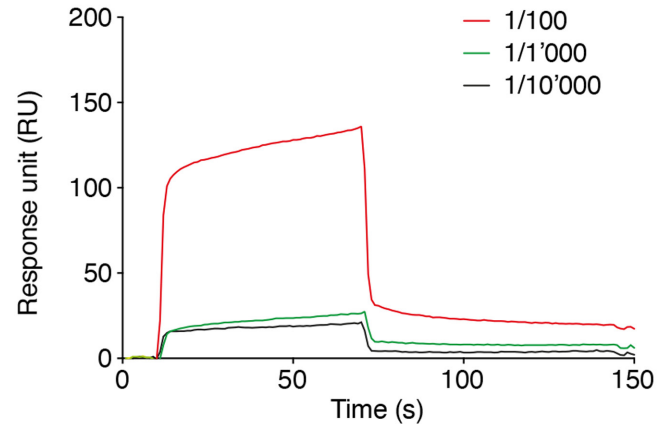
Ia-1 ^{1}VSRGGMRKFIKPLTG^{15}

Ib-1 ^{1}VSRGGMRKKKKPLTG^{15}

(B)

(C)
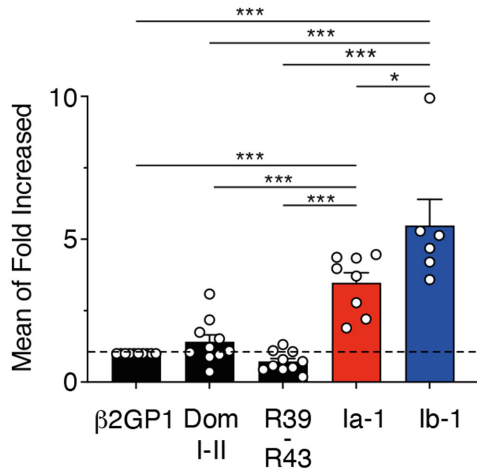
R39-R43-biot

Ib-1-biot ^{1}VSRGGMRKKKKPLTG^{15}

(D)
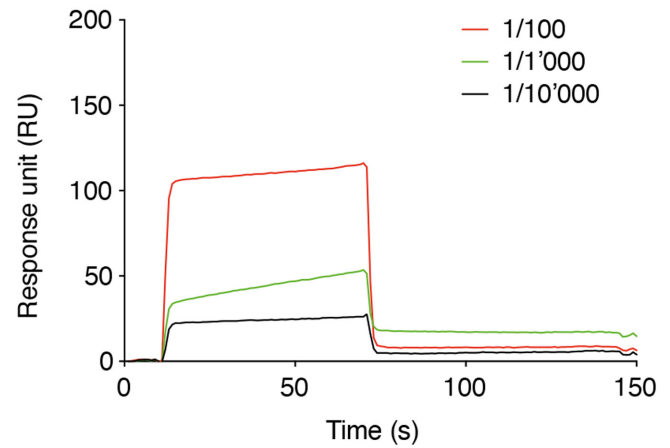
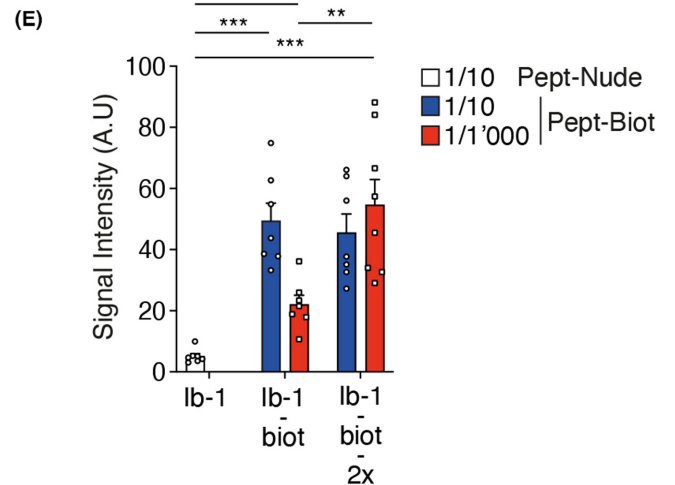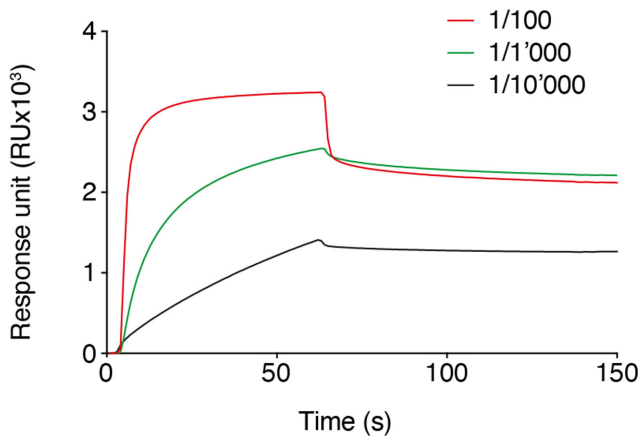Ib-1-biot-2x (^{1}VSRGGMRKKKKPLTG^{15})$_2$

(E)

FIGURE 3 Legend on next page

FIGURE 3 Epitope recognized by aPL requires to be spatially oriented for optimal interactions – (A) Functional evaluation with reduced β2GP1 (β2GP1), Domain I-II of β2GP1 (Dom I-II), peptide R39-R43, and peptide Ia-1 and Ib-1 of aPL at 1/10 dilution of aPL pool. Data are represented in mean of fold increased±SEM relative to interaction level with reduced β2GP1 (β2GP1) ($n = 9$). (B) Function comparison between interactions of biotinylated- (Pept-Biot) and nude-peptide (Pept-Nude) with aPL at 1/10 and 1/1000 dilution of aPL pool ($n = 9$). (C) Quantification of aPL interactions at 1/100, 1/1000, and 1/10,000 dilution with β2GP1 wild-type epitope (R39-43-biot) (upper panel) and monomeric peptide Ib-1-biot (bottom panel) by surface plasma resonance. Representative graph of three independent experiments. (D) Quantification of aPL interactions at 1/100, 1/1000, and 1/10,000 dilution with dimeric peptide Ib-1-biot (bottom panel) by surface plasma resonance. Representative graph of three independent experiments. (E) Function comparison between interactions of monomeric (Ib-1-biot) and dimeric peptide (Ib-1-biot-2x) and nude-peptide (Ib-1) (Pept-Nude) with aPL at 1/10 and 1/1000 dilution of aPL pool ($n = 9$). The nonparametric Mann–Whitney U test was used for statistical analysis: $*p \leq 0.05$; $**p \leq 0.005$; $***p \leq 0.0005$. All data represent mean±SEM

fragments present on aPL. SPR experiments performed with Ib-1-biot-2x-coated chip surface and aPL show an avidity increase of 47.8× and 48.9× at dilution of 1/1000 and 1/10,000, respectively, than the avidity for Ib-1-biot (Figure 3D). At higher concentration (i.e., dilution of 1/100), the avidity for dimeric peptide is 28× more than for the monomeric (Figure 3D). Although the association of two epitopes leads to stronger interaction, the sustained stability of binding is also significantly increased, as we can observe through the shape of the curves (Figure 3D). The dimeric peptide Ib-1-biot-2x thus shows a stronger ability to retain aPL enhancing the signal of 2.48× in comparison with the monomeric form, Ib-1-biot at a dilution of 1/1000 (Figure 3E).

3.3 | Surrounding part of epitope-determining sequence for aPL is essential for the proper interactions with epitope

We have performed a peptide substitution scan of Ib-1-biot VSRGGMRKKKKPLTG carrying the optimized epitope Ib-1-biot and based on an exchange of the underlined amino acid positions with the 20 main amino acids. The resulting peptide microarrays contained 140 different peptides. We observed that the peptide substitution of the positions 1, 2, 12, and 15 (Figure 4A) has a significant influence on the ability to interact with aPL from patients 1, 2, 3, and 4 and, in particular, from the plasma pool. Indeed, the substitution of the position 1, 12, or 15 by an arginine (R) or a lysine (K) increases the affinity of the peptide for all aPL from patients (Figure 1A). However, from the number of identified peptides showing the higher enhancement of aPL interactions (Figure 4B), it seems that no individual mutations displayed a substantial improvement more than any another. In this context, we

evaluated the enhancement relative to Ib-1.0-biot-2x of identified peptides (Figure 4C). The peptides Ib-1.0-biot-2x, Ib-2.0-biot-2x, IIa-5.0-biot-2x, IIa-7.1-biot-2x, and IIa-8.0-biot-2x have the ability to interact with aPL, which is significantly increased with at least three of the four dilutions. Although the sequence IIa-3.1-biot-2x presents a significant increase at a dilution of 1/7500 and 1/60,000, the increase is not enough to be selected because we can also appreciate with the peptide IIa-1.0-biot-2x and IIa-4.0-biot-2x (Figure 4C). However, in streptavidin, known to produce unspecific binding, we used the ratio between aPL and a pool of human plasma as control (B/B0) (Figure 4D, upper panel). This representation therefore allows us to distinguish the real levels of interactions. We then performed a dilution assay from dilution of 1/100 to 1/1,200,000 and observed relevant differences between the different identified peptides. By comparing the area under the curve (AUC), we were able to detect the most prone-interacting peptide with aPL. Thus, the peptide IIa-8.0-biot-2x obtained the higher AUC (Figure 4D, bottom panel). To formally quantify the ability of aPL to interact with IIa-8.0-biot-2x, we measured by flowing various concentrations of aPL over a IIa-8.0-biot-2x-coated chip surface (Figure 4E). These SPR experiments, performed with IIa-8.0-biot-2x-coated chip surface, show that the avidity of aPL is 1.3× more at all dilutions than its avidity for Ib-1.0-biot-2x (Figure 4E, upper panel, and 3D). The sustained stability of binding is also significantly increased as we observed through the shape of the curves (Figure 4E, upper panel). In Figure 4E, bottom panel, we can appreciate more precisely the enhancement of the quality of interactions. Indeed, AUC is 2.3×, 3.43×, and 10.5× higher with IIa-8.0-biot-2x than with Ib-1.0-biot-2x at dilutions of 1/100, 1/1000, and 1/10,000, respectively (Figures 3D, 4E, bottom panel). Last, we can observe that AUC for peptide IIa-8.0-biot-2x is more than 10× the value obtained with the initial target

FIGURE 4 Surrounding part of epitope-determining sequence for aPL is essential for the proper interactions with epitope. (A) Graphical representation of peptide substitution scan microarray performed on VSRGGMRKKKKPLTG with four different aPLs (patients 1, 2, 3, and 4) and a pool of 11 patients (Pool) at 500 μg/ml. (B) Seven identified peptides with higher avidity for aPL. (C) Functional evaluation with identified peptides at indicated dilutions of aPL pool. Data are represented as mean of fold increased±SEM relative to interaction level with Ib-1-biot-2x (Ib-1.0-biot-2x). (D) Upper panel, dilution assay with selected peptides. Data are represented in mean of B/B0 (signal of aPL [aPL pool sera]/signal of pool of plasma from healthy donors)±SEM. Dotted-line = 3× SD of signal for 1/1000 R39-R43 ($n = 10$). Bottom panel, quantification of AUC relative to responses of each peptide. (E) Quantification of aPL interactions at 1/100, 1/1000, and 1/10,000 dilution with peptide IIa-8.0-biot-2x (upper panel) and monomeric peptide Ib-1-biot (bottom panel) by surface plasma resonance. Representative quantification of AUC relative to responses of aPL to β2GP1 wild-type epitope (R39-43-biot), Ib-1-biot-2x and IIa-8.0-biot-2x (bottom panel). The nonparametric Mann–Whitney U test was used for statistical analysis: $*p \leq 0.05$; $**p \leq 0.005$; $***p \leq 0.0005$. All data represent mean±SEM

(A)

Signal Intensity (A.U)

Pool of Patients
Patient 1
Patient 2
Patient 3
Patient 4

(B) Identified Peptides

Ib-1.0-biot   VSRGGMRKKKKKPLTG
Ib-2.0-biot   VSRGGMRKRKKPLTG
IIa-1.0-biot VSRGGMRKKKKKPLTK
IIa-3.1-biot VSRGGMRKKKKKKTG
IIa-4.0-biot RSRGGMRKKKKKPLTG
IIa-5.0-biot VSRGGMRKRKKPLTK
IIa-7.1-biot VSRGGMRKRKKKTG
IIa-8.0-biot RSRGGMRKRKKPLTG

(C)

(D)

(E)

IIa-8.0-biot-2x (^{1}RSRGGMRKRKKPLTG^{15})$_2$

(i.e., R39-43). Altogether, these results demonstrate that aPL from human patients, although recognizing R39–R43 epitope on β2GP1, has a stronger affinity for an epitope rich in arginine (R) and lysine (K), which are present in crucial locations along the sequence.

3.4 | Levels of circulating IgG anti-8.0-biot-2x in lupus-prone mouse model are strongly correlated with clinical manifestation of APS

Our research group has recently studied the mechanism leading to higher cardiovascular mortality in SLE. In this context, we investigated the association between IgG autoantibodies, atherosclerotic parameters, and plaque vulnerability. To address this issue, we crossed the lupus-prone Nba2.Yaa mouse model with atherosclerosis-prone apoE$^{-/-}$ mice, thus generating a mouse model (apoe$^{-/-}$.Nba2.Yaa) that enabled the in vivo study of the potential relation between IgG autoantibodies and atherosclerotic plaque vulnerability.[13,14] APS occurs alone or in association with other autoimmune diseases, particularly SLE (i.e., 30%–50% of SLE patients have APS).[15–17] We have thus investigated whether a lupus-prone mouse model carried IgG anti-IIa-8.0-biot-2x in correlation with other IgG autoantibodies as well as clinical manifestations of APS and atherosclerotic plaque vulnerability. We have measured the levels of IgG autoantibodies against dsDNA, ApoA1, and IIa-8.0-biot-2x (Figure 5A). As mentioned in our previous article,[14] the levels of IgG anti-dsDNA and IgG anti-ApoA1 are increased in apoe$^{-/-}$.Nba2.Yaa in comparison with apoe$^{-/-}$ mice. Beyond the fact that IgG anti-IIa-8.0-biot-2x is also significantly produced by apoe$^{-/-}$.Nba2.Yaa, identified peptide IIa-8.0-biot-2x is able to interact also with aPL produced by mice (Figure 5A). Interestingly, the productions of IgG anti-dsDNA and anti-ApoA1 are strongly correlated with IgG anti-IIa-8.0-biot-2x (Figure 5B), although no cross-reactivities between these antibodies have been observed (data not shown). Other typical clinical manifestations of APS are inversely correlated with the presence of IgG anti-IIa-8.0-biot-2x. Our data indicate that the counts of platelets and red blood cells are low when the concentration of IgG anti-IIa-8.0-biot-2x is high (Figure 5C), although these clinical manifestations are known as extra-criteria manifestations.[18] These effects could be also noticed concerning kidney and mice weight (Figure 5D). Interestingly, a correlation between IgG anti-IIa-8.0-biot-2x concentration and the weight of the spleen and lymph nodes is also observed (Figure 5D). With regard to the atherosclerotic plaque vulnerability parameters, fibrous cap thickness, total collagen, and circulating pro-MMP9 are inversely correlated with the level of IgG anti-IIa-8.0-biot-2x (Figure 5E). Our data indicate that IgG anti-IIa-8.0-biot-2x is highly relevant as an APS biomarker through a good correlation with all clinical manifestations and anti-β2GP1 IgG. They further show that IgG anti-IIa-8.0-biot-2x is potentially relevant for cardiovascular risk similar to anti-ApoA-1 IgG associated with a higher prevalence and incidence of coronary artery disease. In conclusion, this new diagnostic tool based on identified peptide IIa-8.0-biot-2x could provide a better accurate diagnostic, improving the medical management of APS.

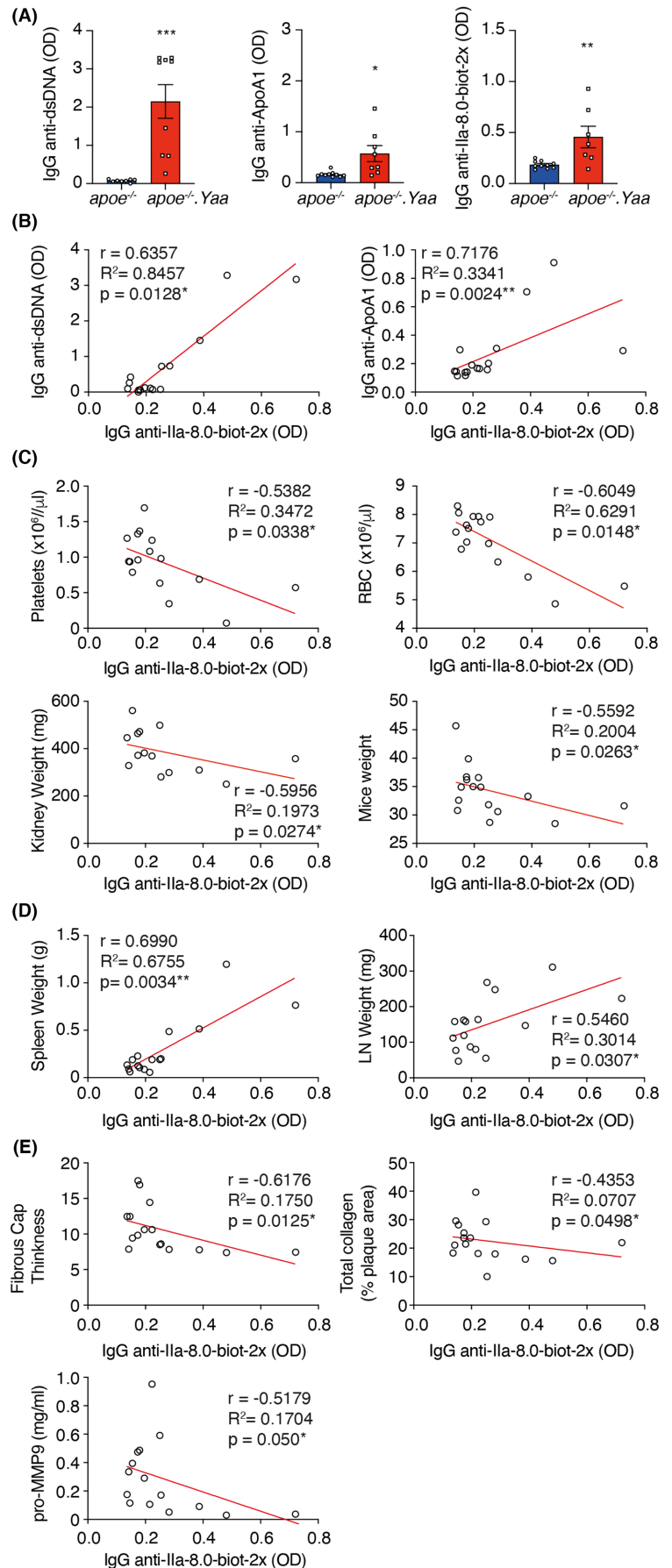## 3.5 | Monoclonal IgG antibody generated with anti-8.0-biot-2x for the standardization of ELISA

To develop a fully standardized ELISA and to confirm anti-IIa-8.0-biot-2x as the epitope of aPL conferring their proinflammatory properties, we generated a monoclonal IgG antibody in mice (14B10). To formally quantify the ability of 14B10 to interact with IIa-8.0-biot-2x, we monitored this result by flowing various concentrations of 14B10 over a IIa-8.0-biot-2x-coated chip surface (Figure 6A). These SPR experiments performed with IIa-8.0-biot-2x-coated chip surface show that the constant of dissociation (K_d) of 14B10 is 180 pM (Figure 6A), classifying this monoclonal IgG antibody among the very high-affinity antibodies for IIa-8.0-biot-2x. Consistent with the results obtained in Figure 3C,D, the antibody 14B10 is also able to bind to the epitope R39-R43 with the similar affinity than the aPL (Figures 3C,6B). We can extrapolate from the sensorgram that aPL from APS patients has a constant of dissociation close (K_d) to 8.9 μM classifying aPL antibody among low- to medium-affinity antibodies for R39-R43 (Figure 6B). We then determined the best standard curve with 14B10 antibody. As seen in Figure 6C, the dynamic range of 800 ng/ml–50 pg/ml is high and the cutoff value (red dotted line) is present in the linear part of the curve (Figure 6C, box). Based on this standardization curve and 236 healthy donors, a cutoff value of 9.50 μg/ml corresponding to the 99th percentile has been determined (Figure S1). Altogether, these data demonstrate that antibody 14B10 IgG has a high affinity and avidity for IIa-8.0-biot-2x but, although monoclonal, is also able to specifically bind the epitope R39-R43 with low affinity. Last, the standard curve performed with 14B10 shows a good dynamic range leading to fully standardized indirect immunoassay for the detection of anti-β2GP1 IgG.

3.6 | Dimers and monomers of IIa-5.0, IIa-7.1 and IIa-8.0 peptides are able to inhibit the binding activity of aPL in vitro

To examine the functional ability of IIa-5.0, IIa-7.1, IIa-8.0 peptides and R39-R43 to inhibit the activity of pool of aPL isolated from APS patients, we evaluated the remaining reactivity of aPL for IIa-8.0-biot-2x, which had previously been treated with increasing concentration of peptides. Although the treatment of aPL with monomeric peptides IIa-5.0, IIa-7.1, and IIa-8.0 prevents their further binding to IIa-8.0-biot-2x ELISA (Figure 7A), the incubation of aPL with dimer of IIa-5.0-2x, IIa-7.1-2x, and IIa-8.0-2x have no effect on aPL ability to interact with IIa-8.0-biot-2x ELISA (Figure 7B). Of note, the monomeric peptide R39-R43 failed to significantly inhibit the interaction of aPL with IIa-8.0-biot-2x ELISA (Figure 7A). As observed in Figure 3, the flag-type orientation prevents potential interactions with the

FIGURE 5 Levels of circulating IgG anti-8.0-biot-2x (anti-β2GP1) in lupus-prone mouse model and Human cohort are strongly correlated with clinical manifestation of APS - Bar graphs represent the median ± SEM. of (A) IgG anti-dsDNA, IgG anti-ApoA-1 and IgG anti-IIa-8.0-biot-2x autoantibody quantification in the serum, measured as optical density (OD) in Apoe$^{-/-}$ or Apoe$^{-/-}$Nba2.Yaa mice on a high cholesterol diet ($n = 8$–10 mice/group). All data were represented as mean ± SEM. The nonparametric Mann–Whitney U test was used for statistical analysis: *$p ≤ 0.05$; ***$p ≤ 0.0005$. Spearman's rank correlation coefficients between IgG IIa-8.0-biot-2x and IgG anti-dsDNA or IgG anti-ApoA-1 (B), Platelets, red blood cells, kidney, and mice weight (C), kidney and mice weight (D), and Fibrous cap thickness, total collagen and pro-MMP9 (E). All data were represented as mean ± SEM. The nonparametric Mann–Whitney U test was used for statistical analysis: *$p ≤ 0.05$; **$p ≤ 0.005$; ***$p ≤ 0.0005$
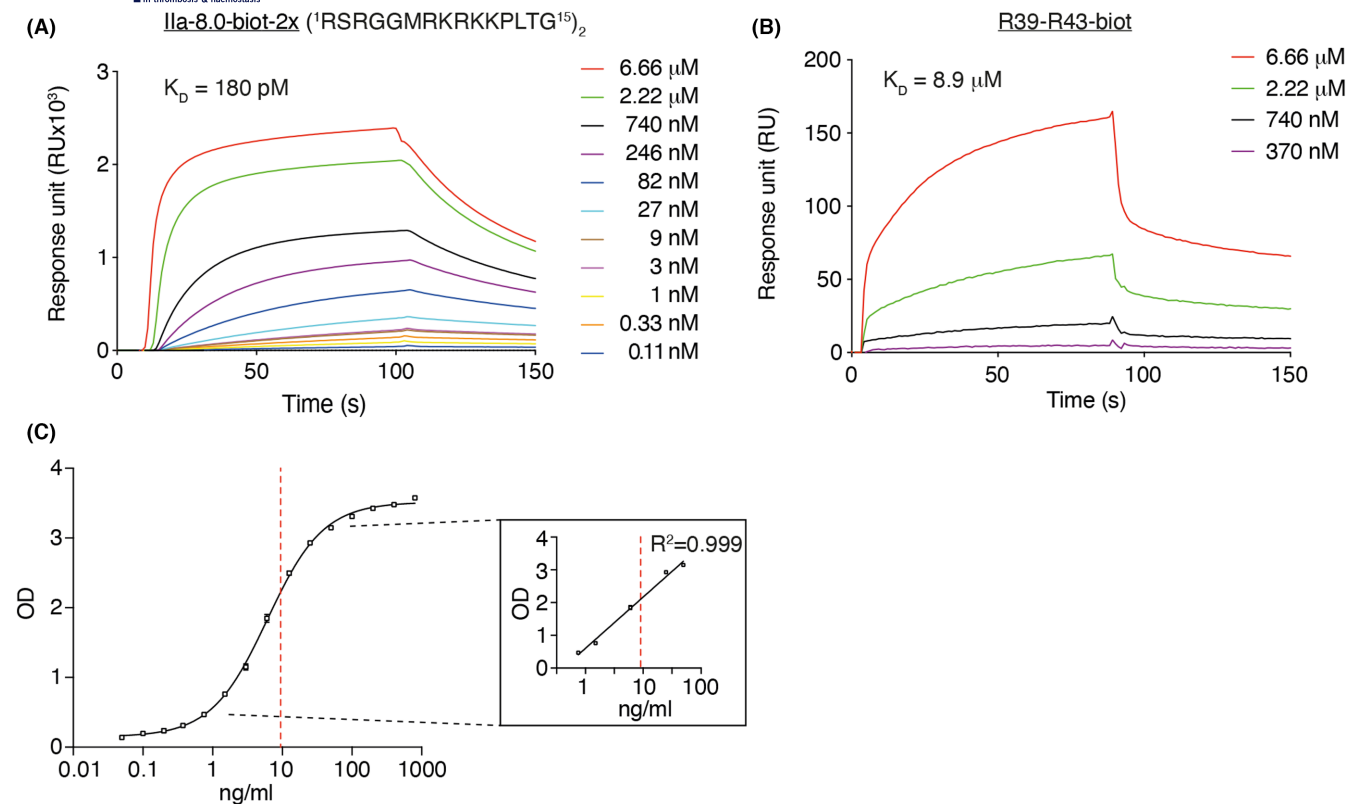
FIGURE 6 Monoclonal IgG antibody generated with anti-8.0-biot-2x for the standardization of ELISA. Quantification of aPL interactions at 6.66 μM to 0.11 nM range of concentration with peptide IIa-8.0-biot-2x (A) or with R39-R43-biot peptide (B) by surface plasma resonance. (C) Dynamic range of the calibration curve with the 14B10 monoclonal antibody. Outlined part of the graph is enlarged for linear portion of standard curve. Red dotted line corresponds to 99th percentile as a cutoff for detection of anti-β2GP1 IgG

plate or with itself, particularly in solution. We have thus generated streptavidin-magnetic beads associated with IIa-5.0-biot-2x, IIa-7.1-biot-2x, and IIa-8.0-biot-2x peptides. We have then treated aPL with increasing concentrations of beads previously to measure the remaining binding activity of aPL on IIa-8.0-biot-2x ELISA (Figure 7C). We observed that the ability of aPL to interact with IIa-8.0-biot-2x is dose dependently inhibited by peptide-associated beads (Figure 7C). These results further confirm the importance of the orientation for efficient interactions with pathogenic aPL.

In 1994, Hunt and Krilis described Domain V of β2GP1 as being responsible for the induction of pathogenic aPL.[19] Domain V has a sequence of 15 amino acids (GDKV) rich in lysines in the PL-binding site, which is able to induce the production of aPL.[20] Based on this

observation, they performed a database searched in the GenBank for some viral and bacterial peptides that have similarities with GDKV.[21] At least three viral and bacterial peptides with sequences similarity to the GDKV-binding region of β2GP1 have been revealed[20]: (1) TADL, Thr_{77}–Glu_{96} of the 72-kDa human adenovirus type 2 DNA-binding protein; (2) TIFI Thr_{101}–Thr_{120} of ULB0-HCMVA from human cytomegalovirus; (3) VITT, Val_{51}–Ile_{70} of US27-HCMVA; and (4) GDKV2 is a modified version of GDKV in which all six residues between Lys_{282} and Lys_{287} were replaced with Lys (Figure 7D–G). Although the similarity between GDKV and TIFI is 58.82%, this correspondence between TIFI and IIa-7.1-biot, IIa-8.0-biot, and IIa-5.0-biot are 66.66%, 46.66%, and 49.66%, respectively (Figure 7D,E). GDKV2 binds aPL more strongly than GDKV[22] and has 73.33%,

FIGURE 7 Optimized peptides are able to inhibit the binding activity of aPL in vitro. (A) Quantification of reactivity against peptide IIa-8.0-biot-2x of aPL pool sera previously incubated with increasing concentration of monomeric IIa-5.0, IIa-7.1, and IIa-8.0 peptides. All data represent mean ± SEM (n = 3–4). (B) Quantification of reactivity against peptide IIa-8.0-biot-2x of aPL pool sera previously incubated with increasing concentration of dimeric IIa-5.0-2x, IIa-7.1-2x, and IIa-8.0-2x peptides (n = 3). (C) Quantification of reactivity against peptide IIa-8.0-biot-2x of aPL pool sera previously incubated with increasing concentration of dimeric IIa-5.0-2x-, IIa-7.1-2x-, and IIa-8.0-2x-associated beads. All data represent mean ± SEM (n = 3). The nonparametric Mann–Whitney U test was used for statistical analysis: *$p \leq 0.05$; **$p \leq 0.005$. (D–G) Sequence alignment with between IIa-5.0, IIa-7.1, and IIa-8.0 with GDKV, GDKV2, TADL, VITT, and TIFI peptide. Black line indicates position with fully conserved residue; light dotted line indicates conservations between residues with strongly similar properties (>0.5 in the Gonnet PAM 250 matrix). Dark dotted line indicates conservations between residues with weakly similar properties (≤0.5 and >0 in the Gonnet PAM 250 matrix). Identity has been calculated by considering only fully conserved residues while Similarity has been calculated by considering all similar properties. All data were represented based on rules of Multiple Sequence Alignment Clustal Omega

(A) IIa-8.0-biot-2x Reactivity

(B) IIa-8.0-biot-2x Reactivity

(C) IIa-8.0-biot-2x Reactivity
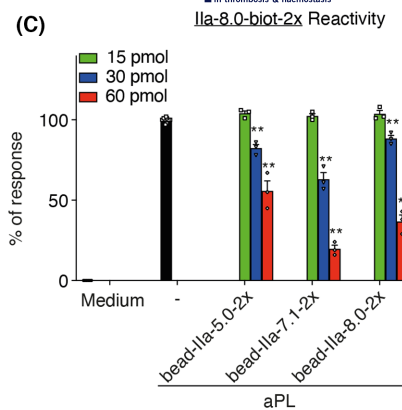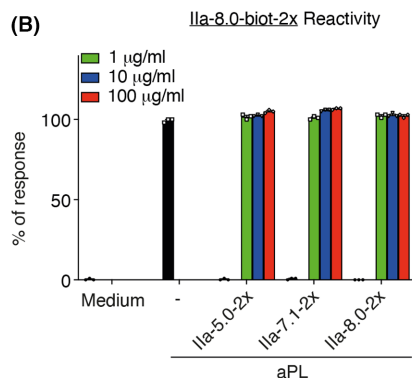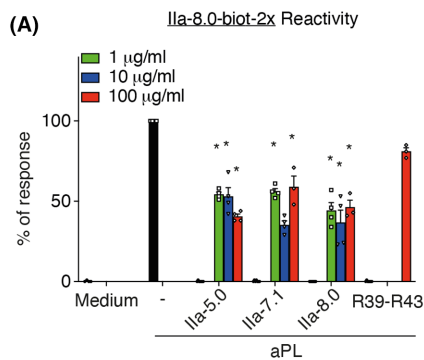
(D)

		Identity:	Similarity:
TIFI	-TIFILFCCSKEKRKKKQAAT	5/17	10/17
GDKV	GDKVSFFCKNKEKKCSY----	29.41%	58.82%

(E)

		Identity:	Similarity:
IIa-7.1-biot	----VSRGGMRKRKKKKTG--	5/15	10/15
TIFI	TIFILFCCSKEKRKKKQAAT-	33.33%	66.66%
IIa-8.0-biot	---RSRGGMR-KRKK--PLTG	5/15	7/15
TIFI	TIFILFCCSKEKRKKKQAAT-	33.33%	46.66%
IIa-5.0-biot	------VSRGGMRKRKKPLTK	4/15	7/15
TIFI	TIFILFCCSKEKRKKKQAAT-	26.66%	46.66%

(F)

		Identity:	Similarity:
IIa-7.1-biot	VSR-GGMRKRKKKK-TG	4/15	11/15
GDKV	GDKVSFFCKNKEKKCSY	26.66%	73.33%
IIa-8.0-biot	RSRGGM-RK-RKKPLTG	2/15	9/15
GDKV	GDKVSFFCKNKEKKCSY	46.66%	60.00%
IIa-5.0-biot	---VSRGGMRKRKKPLTK	5/15	7/15
GDKV	GDKVSFFCKNKEKKCSY-	33.33%	46.66%

		Identity:	Similarity:
IIa-7.1-biot	VSRGG-MRKRKKKK-TG	5/15	11/15
GDKV2	GDKVSFFCKKKKKKKCSY	33.33%	73.33%
IIa-8.0-biot	RSRGG-M-RKRKKPLTG	3/15	10/15
GDKV2	GDKVSFFCKKKKKKKCSY	20.00%	66.66%
IIa-5.0-biot	---VSRGGMRKRKKPLTK	5/15	8/15
GDKV2	GDKVSFFCKKKKKK-CSY	33.33%	53.33%

(G)

		Identity:	Similarity:
IIa-7.1-biot	VSRGGMR-KRKKKKTG----	4/15	11/15
TADL	TADLAIASKKKKKRPSPKPE	26.66%	73.33%
IIa-8.0-biot	---RSRGGMRKRKKPLTG--	3/15	9/15
TADL	TADLAIASKKKKKRPSPKPE	20.00%	60.00%
IIa-5.0-biot	---VSRGGMRKRKKPLTK--	4/15	11/15
TADL	TADLAIASKKKKKRPSPKPE	26.66%	73.33%

		Identity:	Similarity:
IIa-7.1-biot	VSRGGMRKRKKKKTG---	5/15	8/15
VITT	VITTILYYRRKKKSPSDT	33.33%	53.33%
IIa-8.0-biot	-RSRGGM-RKRKK-PL-TG	4/15	8/15
VITT	VITTILYYRRKKKSPSDT-	26.66%	53.33%
IIa-5.0-biot	VSRG---GMRKRKKPLTK	5/15	8/15
VITT	VITTILYYRRKKKSPSDT	33.33%	53.33%

66.66%, and 53.33% similarity with IIa-7.1-biot, IIa-8.0-biot, and IIa-5.0-biot (Figure 7F). The two other peptides rich in lysine, TADL and VITT, also have similarities with IIa-7.1-biot, IIa-8.0-biot, and IIa-5.0-biot between 53.33% and 73.33% (Figure 7G). Consequently, we can suggest that the strong avidity of IIa-8.0-2x, IIa-5.0-2x, and IIa-7.1-2x for aPL may be used to reverse pathogenic effects of aPL and treat clinical manifestations of APS.

4 | DISCUSSION

The present study aimed to identify the strongest aPL-binding antigenic determinant based on initial discontinuous R39-R43 epitope of Domain I of β2GP1. Previous publications from our and other research groups suggest that the substitution of residues inside and around the R39-R43 epitope could change the avidity of aPL for these sequences.[7,23,24] We established that the residues between K44 and P48 are critical to increase the avidity for aPL from APS patients. The substitution of these three residues by a lysine or arginine enhanced the avidity of aPL by almost six times. We also demonstrated that the amino acids surrounding the epitope R39-K47 have a function for interacting with aPL. The modification of the sequences -VSR- and -PLTG- could thus influence positively or negatively the binding of aPL. A new important aspect has been revealed for an effective interaction between aPL and the targeted epitopes. Spatial orientation as "seaweed in the current" represents this new aspect. Using the biotin-streptavidin system, the peptide has been attached to the plate by its N-terminal preventing potential contacts with the plate, which could hide the interaction sites. Altogether, these modifications lead to generating a peptide called IIa-8.0-biot-2x, which presents an ability to interact with aPL that is strongly enhanced in comparison with β2GP1, Domain I of β2GP1, or with the peptide containing the R39-R43 epitope. All these properties have led to the development of indirect solid-phase immunoassay able to detect concentrations of anti-β2GP1 IgG 100× smaller than other assays based on R39-R43, β2GP1 Domain I, or full β2GP1.

As previously mentioned, Gharavi et al.[21] have shown that some viral and bacterial peptides with similarities to GDKV (Figure 7D–G) are able to induce the production of aPL and cause thrombosis and activation of endothelial cells.[20,21] Furthermore, they could also inhibit the pathological properties of aPL.[25] Among described peptides, the TIFI peptide is able to reverse anti-β2GP1 IgG-mediated thrombosis in mice and the binding of aPL on β2GP1, whereas only inhibition of aPL binding on β2GP1 has been reported for the other peptides.[20,25] Although there is a protective effect observed with GDKV or TIFI, and attributed to their ability to bind the phospholipids present to cell surface, these effects could be instead a direct inhibition of anti-β2GP1 IgG. In this perspective, it has been shown that recombinant Domain I (DI) and inhibits the binding of aPLs in vitro and that this inhibition is greater with the DI (D8S/D9G) mutant.[24] Although aPL has an higher affinity for peptide IIa-8.0-biot-2x in comparison to the wild-type DI and in regard to the present data, peptide IIa-8.0-biot-2x, IIa-5.0-biot-2x, and IIa-7.1-biot-2x

could be used for specific clinical management of APS. Although this option is very attractive, additional experiments are required to confirm the potential of peptide-based therapy. Indeed, different challenges are associated with peptide-based therapy such as short half-life and fast elimination, oligomerization or hydrolysis, and oxidation.[26] As can be seen, our peptides IIa-8.0-2x. IIa-5.0-2x, and IIa-7.1-2x seem to have tendency for oligomerization demonstrated by the lack of inhibitory effects on aPL in vitro (Figure 7B). This hypothesis is reinforced by recovering the inhibition properties after peptide association with beads (Figure 7C). This association restores what we call "seaweed in the current" spacial conformation. It further confirms the necessity to use scaffold such as albumin-binding domain[27] to generated effective peptide therapy with our optimized peptides. Other alternatives could exist as strategies for abrogation of pathogenic effects of aPL. Agostinis et al. have demonstrated that a non–complement-fixing antibody to β2GP1 is able to prevent the pathological effects of anti-β2GP1 antibodies.[28] Based on this very interesting study, we can reasonably consider the peptides IIa-8.0 for the generation of antibody-like molecules such as minibody for a novel therapy for APS.

Iverson and colleagues demonstrated that the mutation of glycine 40 or arginine 43 leads to the loss of interaction with most aPL.[6] Several other research groups have performed epitope mapping using point mutations of Domain I. They have identified D8, D9, K19, S38, R39, G40, M42, R43, and N56T as residues participating in aPL–DI interactions.[6,23] Because the distance between the mutation have some effects on aPL-β2GP1 interactions, they conclude at a discontinuous epitope.[6,23] Our research group has considered the polarity specific to each amino acid rather than their charge, and this strategy enabled us to identify a unique motif common to all epitope mutations described previously.[7] For example, lysine is a polar and charged residue, whereas glutamine is polar but uncharged. Zager and colleagues demonstrated that epitopes recognized by aPL all contained the φφφζζ part of the motifs.[29] Alongside with the Zager study, we observed that the identified peptides have the φφφζζ pattern, although it corresponds partially to the motif previously described by our group.[7,29] However, the real size of the epitope appears to be 15 residues long or more, characterized by the physical properties of amino acids whose polarity, hydropathy, and steric volume but not by the sequence of residues. Consequently, considering the size of the epitope, 100% of the critical mutations for aPL (i.e., D8, D9, K19, S38, R39, G40, M42 and R43) are located inside the epitope of anti-β2GP1 IgG.

To our knowledge, Ioannou et al. showed for the first time that mutations, next to the R39-43 epitope, could enhance the binding of IgG from APS patients.[23] These results are consistent with the idea exposed in our previous study[7] that the exact association of residues in peptides based on R39-R43 leads to increase aPL avidity for the target(s). Our current data show also that the epitope recognized by aPL is larger than the five residues encompassed in φφφζζ and brings a new insight on the apparent discontinuity of this epitope as said above. It further demonstrates that the mutations D8 and D9 were only the first step for the improvement

of DI variant enhancing the avidity to aPL from patients with APS. Although the mutations D8 and D9 lead to an increase in the binding to aPL of 0.8x,[23] the peptide IIa-8.0-biot-2x increases the binding to aPL of 23.8× in comparison to the wild-type DI (Figure 3B,E). Finally, they show that recombinant DI inhibits the binding of aPL in the fluid phase to immobilized native antigen, and that this inhibition is greater with the double mutant (D8S/D9G). An *in vivo* study from Pierangeli's group has shown that IgG from APS patients injected into mice significantly increased thrombus size compared with control IgG.[24] This thrombus formation was abolished in mice pretreated with the double mutant (D8S/D9G).[24] Considering the stronger avidity of IIa-8.0-biot-2x in comparison to D8S/D9G, we can reasonably speculate that IIa-8.0-biot-2x represents a potential future therapeutic agent for APS.

The notion of spatial arrangement takes on particular interest when we consider β2GP1. Actually, two different conformations are described for β2GP1: a circular plasma conformation in which domain I interacts with domain V and an "activated" fishhook-like conformation.[4] This fishhook-like conformation is very important for R39-43 cryptic epitope exposure and is critical for binding of pathogenic aPL.[4] The identification of a lysine-rich region next to the R39-R43 epitope is consistent with the conclusion of de Groot's laboratory, suggesting that interactions between the positive charge of this epitope and the negative charge of a hydrophilic ELISA plate may hamper interaction of antibodies with that epitope.[12] Although they further confirmed that exposure of R39-R43 epitope in anti-β2GP1 immunoassays is dependent of coating strategies, de Groot's data have been also established by several other groups.[30–34] To prevent the problems concerning the microplate surface, we have settled spatial orientation as "seaweed in the current" to avoid the potential interactions between our charged peptide and the plates or the peptide oligomerization. Furthermore, generation of monoclonal IgG antibody against IIa-8.0-biot-2x for the standard curve makes of our immunoassay for anti-β2GP1 IgG a fully standardized ELISA.

In summary, this study provides explanations for previous results obtained by many different research groups. Our results demonstrate that sequences with the highest aPL-binding activity possess a length of 15 residues, with a lysine-rich region. We further determine that spatial orientation prevents the interactions between peptide and plate surface is required for an effective detection of aPL. Finally, with superior aPL-binding properties, the peptide IIa-8.0-biot is a serious candidate for specific clinical management of APS.

AUTHOR CONTRIBUTIONS

K.J.B. and M.M. conceived, designed, and supervised the study. M.M., F.B., A.R., D.B., and K.M. performed the experiments. K.J.B., M.M., N.V., F. Montecucco, and F. Mach analyzed the data. K.J.B., M.M., and F. Mach wrote the paper.

ACKNOWLEDGMENTS

FUNDING INFORMATION

RELATIONSHIP DISCLOSURE

M.M., K.J.B., and F. Mach are named as co-inventors on a patent related to monomeric and dimeric IIa-5.0, IIa-7.1, and IIa-8.0 peptides. M.M. and K.J.B. are cofounders of Endotelix Diagnostics Ltd. No research funds or honoraria have been paid by Endotelix Diagnostics Ltd. The remaining authors have no conflict of interest to declare.

ORCID

Marc Moghbel https://orcid.org/0000-0002-3974-7406
Karim J. Brandt https://orcid.org/0000-0003-1042-5283

TWITTER

Karim J. Brandt @@BrandtKarim

REFERENCES

1. Giannakopoulos B, Krilis SA. The pathogenesis of the antiphospholipid syndrome. *N Engl J Med.* 2013;368(11):1033-1044.
2. Miyakis S, Lockshin MD, Atsumi T, et al. International consensus statement on an update of the classification criteria for definite antiphospholipid syndrome (APS). *J Thromb Haemost.* 2006;4(2):295-306.
3. de Laat B, van Berkel M, Urbanus RT, et al. Immune responses against domain I of beta(2)-glycoprotein I are driven by conformational changes: domain I of beta(2)-glycoprotein I harbors a cryptic immunogenic epitope. *Arthritis Rheum.* 2011;63(12):3960-3968.
4. Agar C, van Os GM, Morgelin M, et al. Beta2-glycoprotein I can exist in 2 conformations: implications for our understanding of the antiphospholipid syndrome. *Blood.* 2010;116(8):1336-1343.
5. de Laat B, Derksen RH, van Lummel M, Pennings MT, de Groot PG. Pathogenic anti-beta2-glycoprotein I antibodies recognize domain I of beta2-glycoprotein I only after a conformational change. *Blood.* 2006;107(5):1916-1924.
6. Iverson GM, Reddel S, Victoria EJ, et al. Use of single point mutations in domain I of beta 2-glycoprotein I to determine fine antigenic specificity of antiphospholipid autoantibodies. *J Immunol.* 2002;169(12):7097-7103.
7. de Moerloose P, Fickentscher C, Boehlen F, Tiercy JM, Kruithof EKO, Brandt KJ. Patient-derived anti-beta2GP1 antibodies recognize a peptide motif pattern and not a specific sequence of residues. *Haematologica.* 2017;102(8):1324-1332.
8. Brandt KJ, Kruithof EK, de Moerloose P. Receptors involved in cell activation by antiphospholipid antibodies. *Thromb Res.* 2013;132(4):408-413.
9. Brandt KJ, Fickentscher C, Boehlen F, Kruithof EK, de Moerloose P. NF-kappaB is activated from endosomal compartments in antiphospholipid antibodies-treated human monocytes. *J Thromb Haemost.* 2014;12(5):779-791.
10. Tran NL, Manzin-Lorenzi C, Santiago-Raber ML. Toll-like receptor 8 deletion accelerates autoimmunity in a mouse model of lupus

through a Toll-like receptor 7-dependent mechanism. *Immunology.* 2015;145(1):60-70.

11. Madeira F, Park YM, Lee J, et al. The EMBL-EBI search and sequence analysis tools APIs in 2019. *Nucleic Acids Res.* 2019;47(W1):W636-W641.

12. de Laat B, Derksen RH, Urbanus RT, de Groot PG. IgG antibodies that recognize epitope Gly40-Arg43 in domain I of beta 2-glycoprotein I cause LAC, and their presence correlates strongly with thrombosis. *Blood.* 2005;105(4):1540-1545.

13. Kikuchi S, Santiago-Raber ML, Amano H, et al. Contribution of NZB autoimmunity 2 to Y-linked autoimmune acceleration-induced monocytosis in association with murine systemic lupus. *J Immunol.* 2006;176(5):3240-3247.

14. Santiago-Raber ML, Montecucco F, Vuilleumier N, et al. Atherosclerotic plaque vulnerability is increased in mouse model of lupus. *Sci Rep.* 2020;10(1):18324.

15. Cervera R, Serrano R, Pons-Estel GJ, et al. Morbidity and mortality in the antiphospholipid syndrome during a 10-year period: a multicentre prospective study of 1000 patients. *Ann Rheum Dis.* 2015;74(6):1011-1018.

16. Luigi Meroni P, Toubi E, Shoenfeld Y. Are anti-phospholipid syndrome and systemic lupus erythematosus two different diseases? A 10-year late remake. *Isr Med Assoc J.* 2019;21(7):491-493.

17. Beltagy A, Trespidi L, Gerosa M, Ossola MW, Meroni PL, Chighizola CB. Anti-phospholipid antibodies and reproductive failures. *Am J Reprod Immunol.* 2021;85(4):e13258.

18. Sciascia S, Amigo MC, Roccatello D, Khamashta M. Diagnosing antiphospholipid syndrome: 'extra-criteria' manifestations and technical advances. *Nat Rev Rheumatol.* 2017;13(9):548-560.

19. Hunt J, Krilis S. The fifth domain of beta 2-glycoprotein I contains a phospholipid binding site (Cys281-Cys288) and a region recognized by anticardiolipin antibodies. *J Immunol.* 1994;152(2):653-659.

20. Gharavi EE, Chaimovich H, Cucurull E, et al. Induction of antiphospholipid antibodies by immunization with synthetic viral and bacterial peptides. *Lupus.* 1999;8(6):449-455.

21. Gharavi AE, Pierangeli SS, Espinola RG, Liu X, Colden-Stanfield M, Harris EN. Antiphospholipid antibodies induced in mice by immunization with a cytomegalovirus-derived peptide cause thrombosis and activation of endothelial cells in vivo. *Arthritis Rheum.* 2002;46(2):545-552.

22. Matsuura E, Igarashi M, Igarashi Y, et al. Molecular studies on phospholipid-binding sites and cryptic epitopes appearing on beta 2-glycoprotein I structure recognized by anticardiolipin antibodies. *Lupus.* 1995;4(1_suppl):S13-S17.

23. Ioannou Y, Pericleous C, Giles I, Latchman DS, Isenberg DA, Rahman A. Binding of antiphospholipid antibodies to discontinuous epitopes on domain I of human beta(2)-glycoprotein I: mutation studies including residues R39 to R43. *Arthritis Rheum.* 2007;56(1):280-290.

24. Ioannou Y, Romay-Penabad Z, Pericleous C, et al. In vivo inhibition of antiphospholipid antibody-induced pathogenicity utilizing the antigenic target peptide domain I of beta2-glycoprotein I: proof of concept. *J Thromb Haemost.* 2009;7(5):833-842.

25. Ostertag MV, Liu X, Henderson V, Pierangeli SS. A peptide that mimics the Vth region of beta-2-glycoprotein I reverses antiphospholipid-mediated thrombosis in mice. *Lupus.* 2006;15(6):358-365.

26. Hijazi Y. Prediction of half-life extension of peptides via serum albumin binding: current challenges. *Eur J Drug Metab Pharmacokinet.* 2021;46(2):163-172.

27. Nilvebrant J, Hober S. The albumin-binding domain as a scaffold for protein engineering. *Comput Struct Biotechnol J.* 2013;6:e201303009.

28. Agostinis C, Durigutto P, Sblattero D, et al. A non-complement-fixing antibody to beta2 glycoprotein I as a novel therapy for antiphospholipid syndrome. *Blood.* 2014;123(22):3478-3487.

29. Zager U, Lunder M, Hodnik V, et al. Significance of K(L/V)WX(I/L/V)P epitope of the B2Gpi in its (Patho)physiologic function. *EJIFCC.* 2011;22(4):118-124.

30. Pelkmans L, Kelchtermans H, de Groot PG, et al. Variability in exposure of epitope G40-R43 of domain i in commercial anti-beta2-glycoprotein I IgG ELISAs. *PLoS One.* 2013;8(8):e71402.

31. Matsuura E, Inagaki J, Kasahara H, et al. Proteolytic cleavage of β2-glycoprotein I: reduction of antigenicity and the structural relationship. *Int Immunol.* 2000;12(8):1183-1192.

32. Hijiya N, Miyake K, Akashi S, Matsuura K, Higuchi Y, Yamamoto S. Possible involvement of toll-like receptor 4 in endothelial cell activation of larger vessels in response to lipopolysaccharide. *Pathobiology.* 2002;70(1):18-25.

33. Kuwana M, Matsuura E, Kobayashi K, et al. Binding of beta 2-glycoprotein I to anionic phospholipids facilitates processing and presentation of a cryptic epitope that activates pathogenic autoreactive T cells. *Blood.* 2005;105(4):1552-1557.

34. Yamaguchi Y, Seta N, Kaburaki J, Kobayashi K, Matsuura E, Kuwana M. Excessive exposure to anionic surfaces maintains autoantibody response to beta(2)-glycoprotein I in patients with antiphospholipid syndrome. *Blood.* 2007;110(13):4312-4318.

SUPPORTING INFORMATION

Additional supporting information can be found online in the Supporting Information section at the end of this article.